

# Principle and Realization of an ESPAR Antenna Using L and C

Dae-Geun Yang, Eun-Seok Jang, Kyung-Soo Kim, Che-Young Kim, and Sung-Soo Hong  
 School of the Electronics Engineering, Kyungpook National University,  
 Daehak-ro 80, Buk-gu, Daegu 702-701, South Korea

**Abstract -** In this paper, a method for determining the value of the inductor (L) and the capacitor (C) that maximize the channel capacity is presented. An optimized beam steering characteristic is realized through this method. The proposed ESPAR antenna structure is composed of a mono fed, active antenna, and two parasitic antennas. The predetermined L and C are connected to the parasitic antennas. The proposed ESPAR antenna was fabricated and the S-parameter, radiation pattern, and the gain of the fabricated antenna were measured at a resonant frequency of 2.4 GHz. The resultant gain was 3.75 dBi, and it was proved that the MIPP and beam steering characteristics that are the requirements of an ESPAR antenna were realized.

**Index Terms —** ESPAR antenna, MIPP, Channel capacity, MIMO

## 1. Introduction

Of late, the necessity and availability of portable terminals for wireless communication have increased rapidly. As a result, the value of high-speed data transmission for next generation mobile communication systems has significantly increased. As a means of realizing high-speed data transmission, multiple-input multiple-output (MIMO) systems have received significant attention. The MIMO system by the Bell Research Institute has enabled high-speed data transmission using several antennas at the transmitter and receiver to increase the channel capacity [1]. However, conventional MIMO antennas have difficulties in miniaturization because they require a number of RF-chains. Further, a perfect isolation and envelope correlation coefficient are difficult to realize technically. To overcome this problem, an electronically steerable parasitic array radiator (ESPAR) was proposed [2]. The ESPAR antenna is single fed by the active antenna only. The other parasitic antennas are connected to the inductor and the varactor capacitor, and the reactance of the varactor capacitor is varied to steer the beam [3]. Therefore, the reactance value used should be calculated exactly because it is important for the ESPAR antenna; the reflected reactance value should not affect the reflection coefficient and should not cause a power imbalance. Additionally, it has to maximize the channel capacity.

In this paper, we illustrate a technique for the calculation of an appropriate reactance value. A mirror image pattern pair (MIPP) is implemented using a computational method. As a result, the embedded radiation patterns,  $B_1$  and  $B_2$ , are proved orthogonal to each other.

## 2. ESPAR Antenna

The simplest ESPAR antenna is composed of one active antenna and two parasitic antennas. The parasitic antennas are connected to the reactance element to steer the beam. The two steered patterns,  $G_1(\theta, \phi)$  and  $G_2(\theta, \phi)$ , should have a MIPP characteristic.  $G_1(\theta, \phi)$  and  $G_2(\theta, \phi)$  are converted into  $B_1(\theta, \phi)$  and  $B_2(\theta, \phi)$  by equation (1) [2].  $G_1(\theta, \phi)$  and  $G_2(\theta, \phi)$  satisfying equation(1) become the orthogonalized basis patterns that can express the output signal.

$$\begin{aligned} B_1(\theta, \phi) &= \frac{1}{\sqrt{2}}[G_2(\theta, \phi) + G_1(\theta, \phi)] \\ B_2(\theta, \phi) &= \frac{1}{\sqrt{2}}[G_2(\theta, \phi) - G_1(\theta, \phi)] \end{aligned} \quad (1)$$

## 3. Channel capacity

Maximizing the channel capacity is important because the ESPAR antenna is used for large data transmissions. Therefore, the L and C that maximize the channel capacity have to be connected to the parasitic antennas. The formula for the channel capacity is given by equation (2) and its unit is [bps/Hz] [2].

$$S_{av} = \arg \max_{[X_1, X_2]} \left\{ \log_2 \left( 1 + \frac{P_i \Delta_T}{\sigma_n^2} \cdot \frac{r}{(1+r)^2} \right) \right\} \quad (2)$$

In equation (1),  $P_i/\sigma_n^2$  is the SNR,  $\Delta_T$  is  $1 - |\Gamma_{tot}|^2$ , and r is the power imbalance ratio. The S-parameter and radiation pattern are required to determine the reactance value that maximizes the channel capacity.

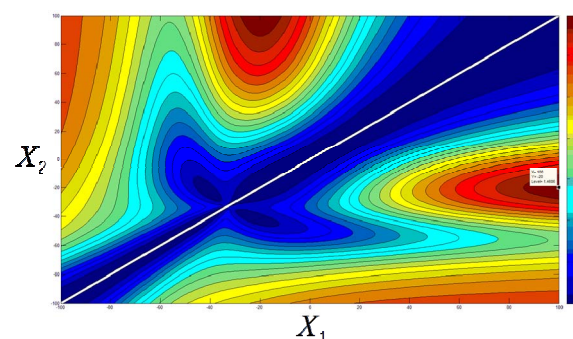


Fig. 1. Channel capacity in terms of  $X_1$  and  $X_2$

The channel capacity contour lines in figure 1 are obtained by substituting these values in equation (1). From the figure, the optimized reactance values are  $X_1 = j100 \Omega$  ( $L=6.8 \text{ nH}$ ) and  $X_2 = -j20 \Omega$  ( $C=3.3 \text{ pF}$ ). The reactance,  $X_1$ , is indicated at the x-axis and the reactance,  $X_2$ , is indicated at the y-axis. Further, as the red ratio increases, the channel capacity increases.

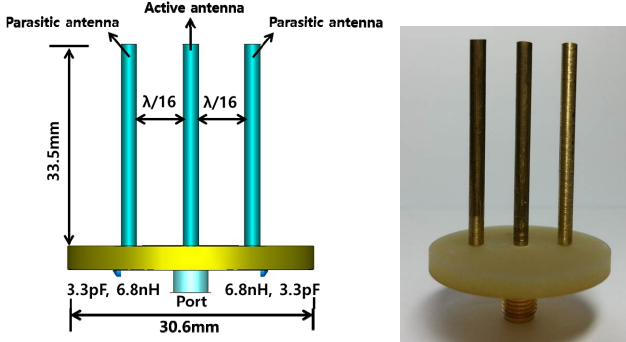


Fig. 2. Geometry and dimensions of the proposed ESPAR antenna

Figure 2 depicts the structure of the ESPAR antenna designed by applying the values of  $L$  and  $C$  that maximize the channel capacity. The distance between each antenna is  $\lambda/16$  and FR-4 is employed as the dielectric substance. The resonant frequency is 2.45 GHz. The  $G_1$  and  $G_2$  patterns given by equation (1) are realized as given below: the  $C$  (3.3 pF) is first connected to the left parasitic antenna and then the  $L$  (6.8 nH) is connected to the right parasitic antenna for obtaining the  $G_1$  pattern, and vice versa for  $G_2$ .

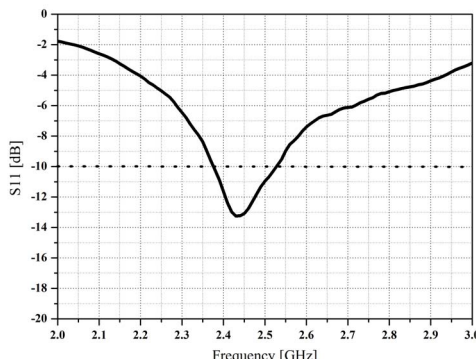


Fig. 3. Measured S-parameter of the fabricated ESPAR antenna

Figure 3 shows the measured  $S_{11}$  of the fabricated ESPAR antenna; the antenna resonates at 2.45 GHz as per the intended design. Figure 4 displays the simulated  $G_1$  and  $G_2$ . The main lobe of the radiation pattern is formulated in the direction of the parasitic antenna connected to  $C$ . This phenomenon is identical in operation to a reflector and an inductor of the Yagi antenna [4]. Figure 5 depicts the measured  $G_1$  and  $G_2$ ; a smooth pattern is observed because the optimized  $L$  and  $C$  that maximize the channel capacity are employed. The MIPP, one of the important

characteristics of the ESPAR antenna is formulated on the pattern and the measured antenna gain is 3.75 dBi.

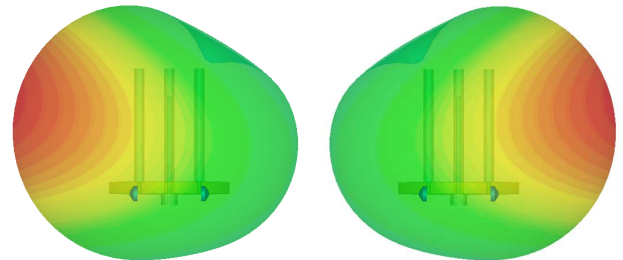


Fig. 4. Simulation results for the radiation patterns ( $G_1, G_2$ )

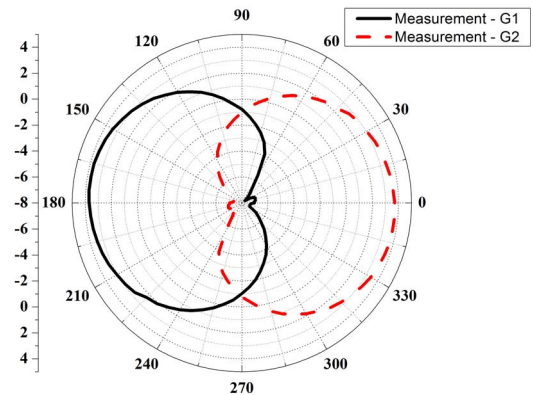


Fig. 5. Measurement results for the gain patterns of the proposed ESPAR

#### 4. Conclusion

In this paper, the theory and design methodology for the ESPAR antenna, a next generation technology, are described. Using this process,  $L=6.8 \text{ nH}$  and  $C=3.3 \text{ pF}$  are computed by a formula, and these values are used to maximize the channel capacity. An antenna based on this method was fabricated and measured. The measured  $S_{11}$  at 2.45 GHz is lower than  $-10 \text{ dB}$  and satisfies a standard; the measured gain is 3.75 dBi. The  $G_1$  and  $G_2$  patterns formulate the MIPP. The proposed antenna to which a single RF-chain is applied, is miniaturized compared to an existing MIMO antenna to which multi RF-chains are applied. By analyzing the measured data, it is also proven that the performance of the proposed antenna is as good as the existing MIMO antenna.

#### References

- [1] Yang, D.G., Kim, D.O., and Kim, C.Y.: ‘Design of dual-band MIMO monopole antenna with high isolation using slotted CSRR for WLAN’, *Microwave Opt. Technol. Lett.*, vol. 56, pp. 2252-2257, 2014.
- [2] Mohsen, Y., Osama, N.A., and Julien, P.C.: ‘Efficient MIMO transmission of PSK signal with a single radio reconfigurable antenna’, *IEEE Trans. Commun.*, vol. 62, pp. 567-577, 2014.
- [3] Osama, N.A., Constantinos, B.P., Antonis, K., Nicola, M., and Ramjee, P.: ‘MIMO transmission and reception techniques using three-element ESPAR antennas’, *IEEE Commun. Lett.*, vol. 13, pp. 236-238, 2009.
- [4] Kim, D.O., and Kim, C.Y.: ‘Dual-band quasi-Yagi antenna with split ring resonator directors’, *Electronics Lett.*, vol. 48, pp. 809-810, 2012.